ZERO-G RADIO FREQUENCY GAGING SYSTEM

FOR SPACE SHUTTLE PROPELLANT TANKS

H. E. Thompson

NASA-Marshall Space Flight Center
Huntsville, Alabama

and

N. E. Stanley, B. J. Shebler, W. Ott

Bendix Corporation
Davenport, Iowa

ABSTRACT

This paper presents the progress of RF Gaging and its applicability to Space Shuttle propellant gaging systems. Included are basic theory, analysis, test results to substantiate theory and analysis, along with test data from systems built and tested to date. Also included are tank and fluid orientation data with characteristic performance curves, repeatability and system accuracy. Some problem areas and their solutions as applicable to space shuttle mission capability enhancement are also presented.

INTRODUCTION

A Radio Frequency mass quantity gaging system is presently being evaluated for application in space vehicle propellant systems. Analysis and substantiating tests have been carried out with various hydrocarbon fuels, liquid oxygen, and liquid nitrogen to determine system performance characteristics over various frequency ranges, fill levels and tank orientations.

Presented in this paper is fundamental description of the principle of operation for RF gaging, along with mathematical formulas and supporting data. Also included are system block diagrams, photographs of hardware and some test setup arrangements. The data presented depicts loading data characteristic curves for various fluids and system gaging accuracy as applicable to Space Shuttle.

BACKGROUND

In 1966 Bendix funded a study program at Iowa State University to determine what basic principles could be used to gage fluids in a Zero-g environment. From this study the Radio Frequency resonant cavity technique was selected as having the best potential.

During early RF gaging development, the technology of microwave and low frequency integrated circuits was not sufficiently advanced to allow use of suitable off-the-shelf components. Therefore, laboratory test equipment and specially designed circuits were relied upon. As components needed to fabricate the necessary circuitry have become state-of-the-art in the last year or so, significant improvements have evolved.

During development of this system, the fundamental relationships between propellant mass and mode count were investigated, including a means for exciting the modes in a more optimum manner. The mode patterns observed as the oscillator frequency was swept over selected frequency ranges, provided experimental data for low-loss and high-loss propellants that could be used to support theoretical analysis. Theoretical Mathematical expressions have advanced that provide a means for calculating the needed operating fre-

quency and the expected number of observable resonant modes in a propellant tank as a function of liquid mass in the tank.

Under the sponsorship of MSFC, further experimental verification and the refinements of theoretical predictions have been recently carried out with good success, and have provided a basis for developing scaling correlations and improved system performance predictions.

PRINCIPLE OF OPERATION

The Radio Frequency (RF) quantity gaging concept envisions the introduction of microwave energy into a tank so as to illuminate it by setting up electromagnetic fields throughout the entire volume of the tank. The tank interior is a dielectric region completely surrounded by conducting walls. There exist electromagnetic field solutions of certain frequencies and spatial configuration that satisfy the boundary conditions and correspond to the storage of electromagnetic energy over time intervals that are long compared with the period of the resonant frequencies. Such a system is commonly called a cavity, and the resonant solutions are the normal theoretical modes of the cavity. Each cavity has a different set of normal modes, differing both in frequency and in spatial configuration. All such sets have an infinite number of members.

If the set of normal modes is ordered with respect to increasing resonant frequency, there is always a lowest resonant frequency, but, in general, no highest resonant frequency. In the direction of higher frequencies, the normal modes increase in complexity and in density, becoming infinitely dense at infinite frequencies. For a given frequency range above the lowest resonant frequency, mode density increases with average dielectric (real part of the complex permittivity) of the cavity.

The number of observable (detectable) modes will be equal to or less than the number of theoretical modes dependent on the following factors: Q of the tank and antenna assembly, complex permittivity of the

average dielectric of the tank, mode detector and the characteristic impedance of the RF source and coupling elements, including RF cables.

If the average dielectric and the walls of the tank were ideally lossless, the density of detectable modes would always increase with frequency. However, due to tank wall losses, even with an ideal lossless dielectric, the density of detectable modes eventually reaches a peak with increasing frequency and then falls off. This is due to normal modes merging when the system Q is less than infinity.

If a low loss dielectric is added to the tank interior, the density of detectable modes will increase at a higher rate with frequency due to the increased real part (ε') of the complex permittivity; however, the peak density will now occur at a lower frequency due to additional loss contributed by the imaginary part ($j\varepsilon''$). With higher loss dielectrics, this phenomena is amplified so that the peak density may occur at relatively low frequencies in the microwave spectrum.

Based on the statistical probability of "observing", or detecting, a mode, an equation has been developed which predicts this type of behavior. Figure 1 is a plot of densities for a high loss dielectric calculated using the equation and plotted versus frequency for several different filling factors. Because the relatively low frequency at which the peak occurs when the tank is full, it is evident that high loss dielectrics should be gaged on the high frequency "tail" of the density curves where the number of modes will be decreasing with increasing frequency. In contrast with this, low loss dielectrics are more conveniently gaged on the low frequency side where the number of modes increases with increasing frequency.

Integration of the mode density curves of Figure 1 over a fixed frequency band produces the number of observable modes in that band. Figure 2 shows the number of modes which exist in selected frequency bands as the tank is filled with RP-1. Also shown is the output voltage which would exist if the number of modes is converted directly to an analog signal.

To obtain a system with detectable modes that are nearly independent of the location of the fluid in the tank, the number of cubic wavelengths at the lowest frequency is made as large as possible by increasing the lower band-edge frequency.

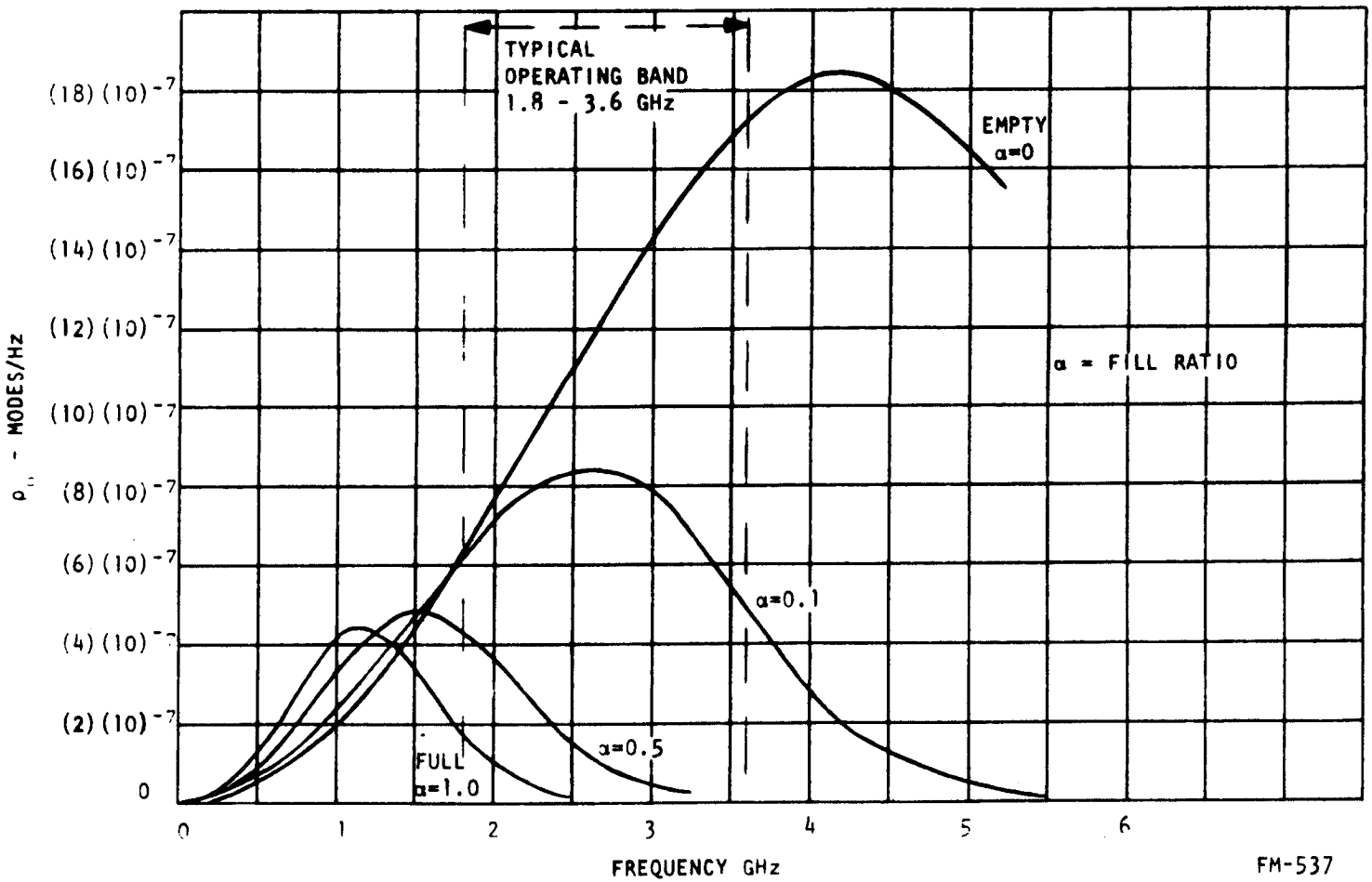

Figure 1.- DENSITY OF OBSERVABLE MODES IN A 1/10-SCALE S-1VB TANK LOADED WITH RP-1

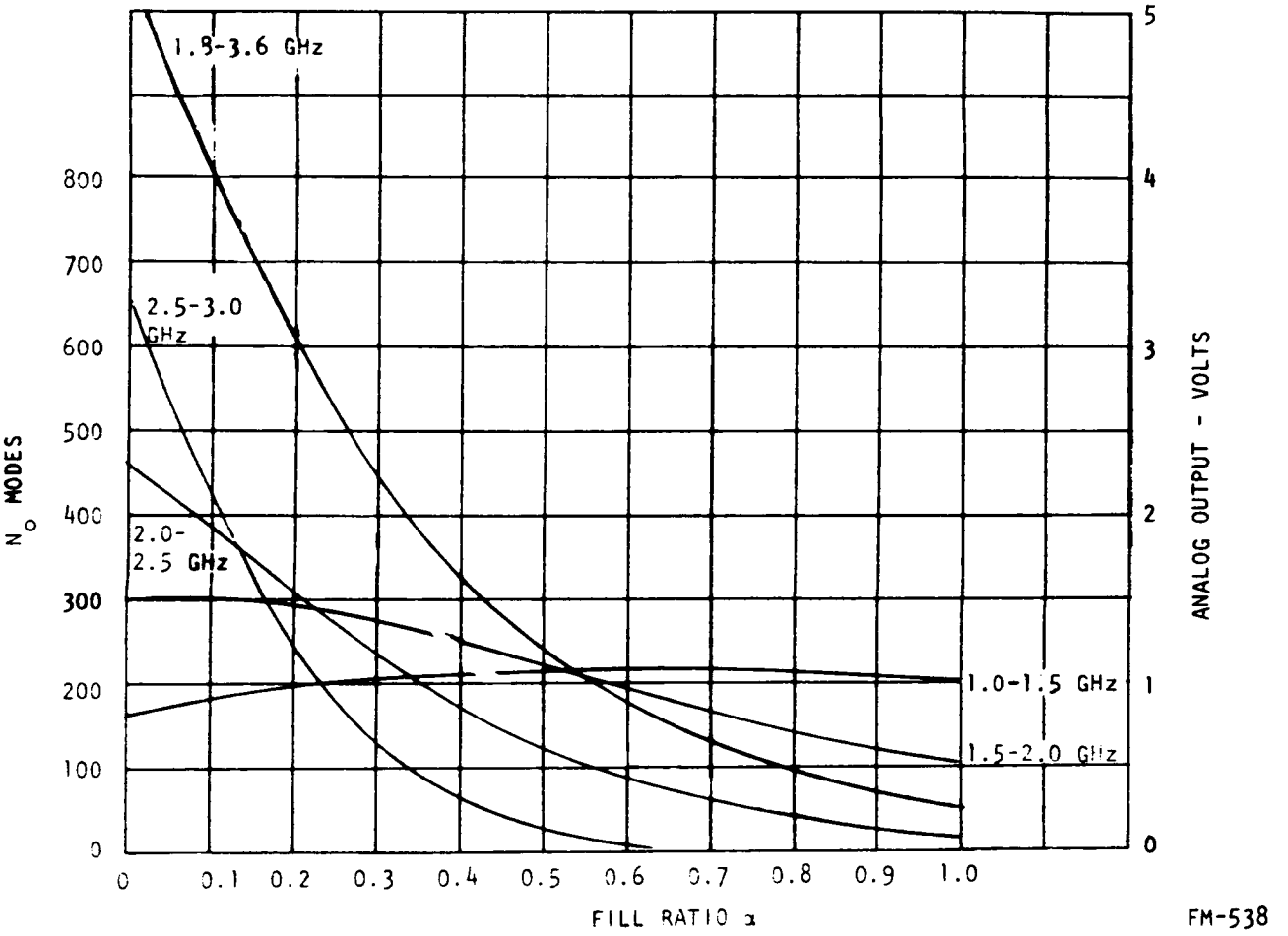

Figure 2.- OUTPUT CHARACTERISTICS OF A RF GAGING SYSTEM ON A 1/10-SCALE S-1VB TANK FILLED WITH RP-1

Figure 3 shows the RF Gaging System in block diagram form. The RF section consists of a voltage tunable RF Sweep Oscillator, an attenuator, a low-pass filter which cuts off at the maximum desired output frequency, and a directional coupler which provides a sample of the RF power level. This level is held constant by detecting it at the directional coupler and using the detected power level to control a power leveling circuit. The power leveling circuit controls the DC bias of the RF sweep oscillator.

The RF oscillator frequency is controlled by a ramp voltage which is generated in the Ramp Generator. The ramp voltage causes the oscillator to sweep over a frequency f_1 to f_2.

The RF energy is coupled into the tank probe through a circulator and coaxial cable. The tank probe is a wide band spiral antenna. The RF energy reflected from the probe is detected at the third port of the circulator using a Mode Detector (crystal diode). This detected energy contains the mode information.

The Signal Processing circuit produces a constant-width, constant-amplitude pulse for each detectable mode. This provides a train of pulses which can be counted electronically by using the timing pulse from the ramp generator, or fed into a Pulse to Analog Converter to obtain an 0-5 VDC analog voltage.

PROGRESS TO DATE

Recent efforts to experimentally evaluate the latest RF gaging refinements have been very successful. Much progress has been made in correlating analytical predictions with experimental results. The calculated operating RF frequency band, and the subsequent number of modes observed for a given tank and fluid can now be made with a greater degree of confidence. Data obtained with laboratory test tanks and test fluids has been shown to be very repeatable on a day-to-day basis, regardless of whether laboratory or prototype RF sources are used.

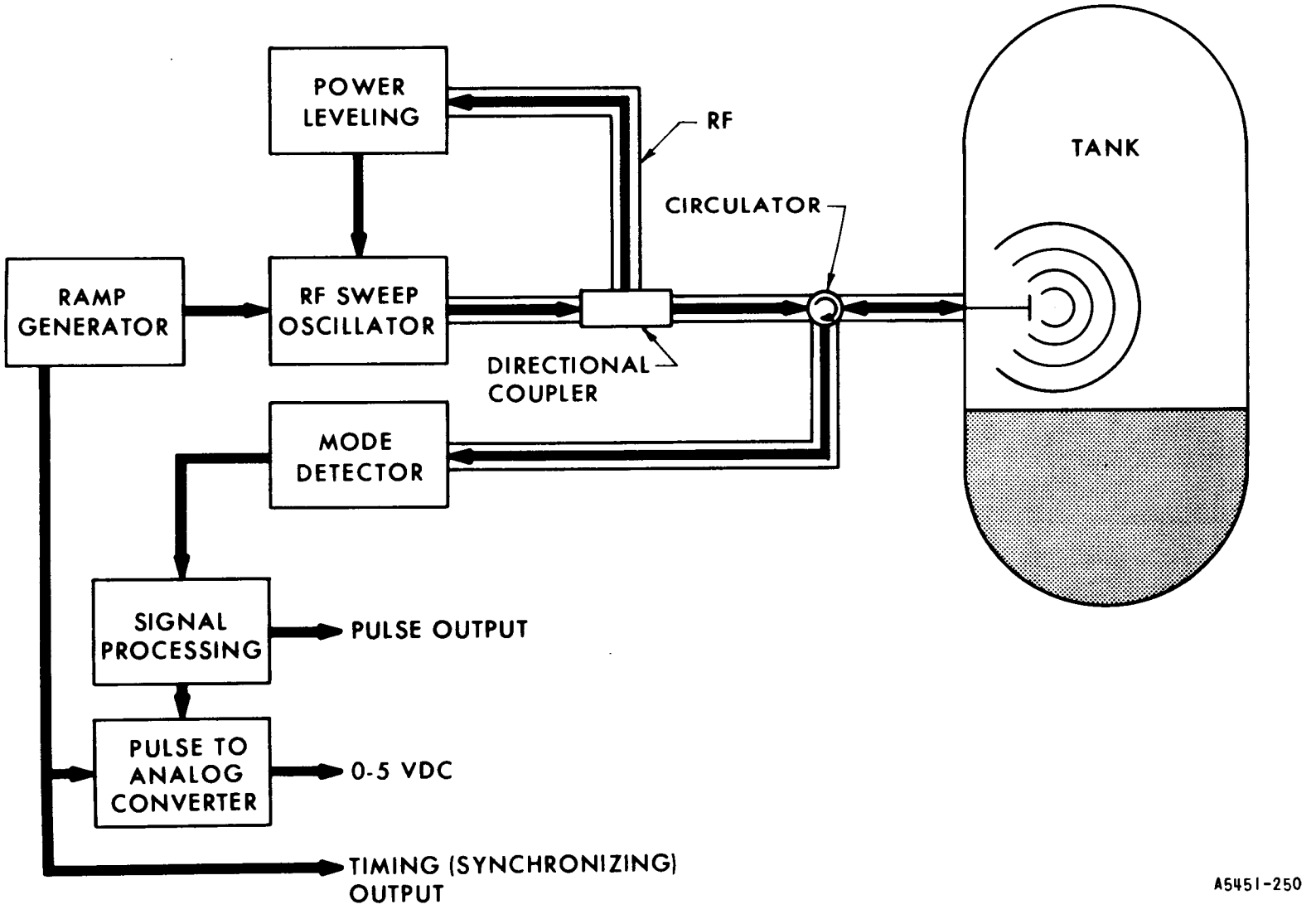

Figure 3.- RF MODE COUNTING SYSTEM

Theoretical Analysis

The theoretical maximum number of modes which may be established for a given empty tank over a fixed frequency band can be expressed mathematically. Over the frequency band bounded by f_1 and f_2, the number of modes that can be excited is given by:

$$N = \frac{8\pi V}{3c^3}\left[f_2^3 - f_1^3\right] \qquad (1)$$

where

V = volume of the tank

c = velocity of light

When the tank is partially filled with a dielectric material, the theoretical mode count loading dependence is a linear relationship given by the following expression:

$$N = \frac{8\pi V}{3c^3}\left\{f_2^3 - f_2^3\right\}\left\{1 + [(\epsilon')^{3/2} - 1]^{\alpha}\right\} \qquad (2)$$

where

ϵ' = the dielectric constant of the material (real part of permittivity)

α = fractional fill ratio

Equation (2) describes the ideal case. In practice it is impossible to excite, detect, and count all the theoretically possible modes in any given tank due to mode degeneracies and mode merging. Mode degeneracy is a condition where more than one mode exists at a given frequency, and is therefore detected and counted as one. Mode merging is defined as the merging of neighboring modes caused by a low system Q. In the case of high Q systems (tanks whose internal surfaces are good electrical conductors, and where the material to be gaged has a low electrical loss factor) Equation (2) can be used to predict the maximum number of excitable modes. Since this number is the maximum possible, not including mode degeneracies, the actual observable mode count falls below this predicted maximum. An empirical modification of Equation

(2) can be made to reflect the effects of mode degeneracy.

A generalized theoretical treatment derived from Equation (2) that takes into account low Q systems in which mode merging is evident has been formulated, and is given by:

$$\rho_o = 3Kf^2 \exp\left(-\frac{2\beta}{Q_L} Kf^3\right) \qquad (3)$$

where

ρ_o = frequency - density of observable modes

$K = \frac{8V}{3c^3}\left\{1 + [(\ )^{3/2} - 1]\right\}$

β = experimental factor

Q_L = quality factor, or Q of system

Equation (3) is based on the statistical probability of mode detection.

The actual number of observable modes, (N_o), in a frequency band from f_1 to f_2 may be obtained by integrating Equation (3) between these limits. This gives:

$$N_o = \frac{1}{C}\left[\exp(-CN_1) - \exp(-CN_2)\right] \qquad (4)$$

where

$C = \frac{2\beta}{Q_L}$

$N_{1,2} = K(\alpha) f_{1,2}^3$

The system Q; Q_L, can be calculated using the formula

$$\frac{1}{Q_L} = \frac{1}{Q_d} + \frac{1}{Q_u} + \frac{1}{Q_i} + \frac{1}{Q_e} \qquad (5)$$

where Q_d (α) relates to the dielectric, Q_u relates to the empty tank, Q_i relates to internal thermal insulation if present, and Q_e relates to the external source and RF probe. The quality factor Q_d

is a function of the fractional fill ratio, α, and dependent on both the real and imaginary parts of the complex permittivity ($\varepsilon' - \varepsilon''j$) of the material to be gaged.

The value of Q_L, as determined from Equation (5), may be used in conjunction with Equation (4) to establish the optimum frequency limits, f_1 and f_2, for a high loss, descending curve of $N_o(\alpha)$.

Table I contains the computed optimum frequency bands for several tanks and fluids. Empirical substantiation of these predictions to establish system scaling law methods is currently being achieved under a NASA MSFC contract.

Test Results

During the past few years a large amount of experimental data has been gathered in which the intended purposes were:

1) To correlate theoretical predictions of loading dependence as determined by Equations (2) and (4) with experimental results and verify scaling relationships.
2) To verify the prediction that the mode count remains essentially invariant with redistribution of the tank contents.
3) To evaluate the RF gaging system under operating conditions that could not be determined theoretically; that is, propellant out-flow, and dynamic situations as simulated by slosh and bubbling conditions.

Testing of the RF gaging system concept to the above objectives has been performed successfully on several scale model spacecraft tanks and with several simulated fuels. Safety and cost considerations have limited testing with LOX and LN_2 to static tests; however, with cryogenics there is presently no reason to believe that orientation sensitivity should be any greater than that of the non-cryogenic fuel simulates.

Fuel simulates such as Benzene and RP-1 have been used for orientation sensitivity tests with data as shown in Figures 4 and 5 repeated several times, indicating very little orientation sensitivity.

TABLE I

FREQUENCY RANGE FOR VARIOUS TANK & FLUID ELECTRICAL PROPERTIES

TANK	FREQUENCY RANGE GHz	LIQUID	VOLUME [m^3]	SURFACE AREA [m^2]	ϵ'	ϵ''	tanδ	N_{oe}	N_{of}
General Space	2.3 to 3.6*	RP-1	0.133	1.55	2.08	$(190)(10)^{-5}$	$(91.5)(10)^{-5}$	1,182	149
1/10 Scale S-IVB	2.0 to 3.0	RP-1	0.220	2.65	2.08	$(190)(10)^{-5}$	$(91.5)(10)^{-5}$	1,107	20
1/20 Scale S-IVB	4.0 to 5.0	RP-1	0.0256	0.628	2.08	$(190)(10)^{-5}$	$(91.5)(10)^{-5}$	438	24
Spherical Al	1.60 to 2.8	RP-1	0.164	1.45	2.08	$(190)(10)^{-5}$	$(91.5)(10)^{-5}$	791	50
Spherical Al	1.5 to 2.4	Transil Oil	0.164	1.45	2.18	$(610)(10)^{-5}$	$(280)(10)^{-5}$	504	7
General Space	4.2 to 5.0	Benzene	0.133	1.55	2.28	$(13.1)(10)^{-5}$	$(5.75)(10)^{-5}$	1220	245
1/10 Scale S-IVB	3.5 to 4.2	Benzene	0.220	2.65	2.28	$(13.1)(10)^{-5}$	$(5.75)(10)^{-5}$	1,256	277
1/20 Scale S-IVB	5.5 to 6.5	Benzene	0.0256	0.628	2.28	$(13.1)(10)^{-5}$	$(5.75)(10)^{-5}$	681	608
1/10 Scale S-IVB	3.0 to 3.8	Styrofoam	0.220	2.65	1.2	$(30)(10)^{-5}$	$(25)(10)^{-5}$	1,314	271
1/20 Scale S-IVB	5.0 to 6.0	Styrofoam	0.0256	0.628	1.2	$(30)(10)^{-5}$	$(25)(10)^{-5}$	604	312
1/10 Scale S-IVB	4.6 to 5.1	Paraffin	0.220	2.65	1.65	$(3.43)(10)^{-5}$	$(2.08)(10)^{-5}$	850	288
1/10 Scale S-IVB	4.7 to 5.2	LN_2	0.220	2.65	1.428	$(4.28)(10)^{-5}$	$(3)(10)^{-5}$	581	154
1/10 Scale S-IVB	2.0 to 3.0	LOX	0.220	2.65	1.51	$(136)(10)^{-5}$	$(90)(10)^{-5}$	1,052	68
Spherical Al	1.6 to 3.0	LOX	0.164	1.45	1.51	$(136)(10)^{-5}$	$(90)(10)^{-5}$	1,010	243
Full Scale S-IVB	0.5 to 1.0	LH_2	300	320	1.23	$<(1)(10)^{-7}$	$<(1)(10)^{-7}$	1,780	1020

*Based on Actual Test Data. All other Ranges Calculated from Equations Given in Appendix A.

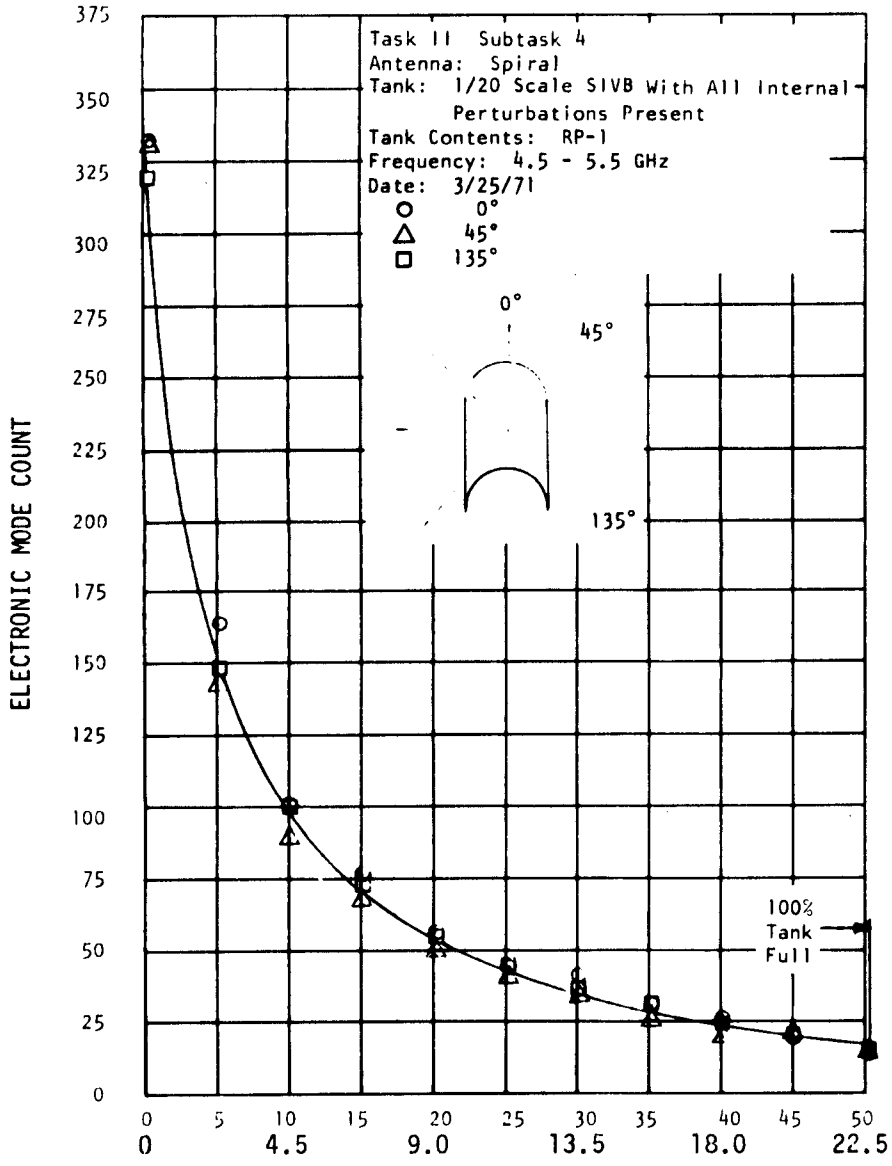

Figure 4.- RP-1 MASS

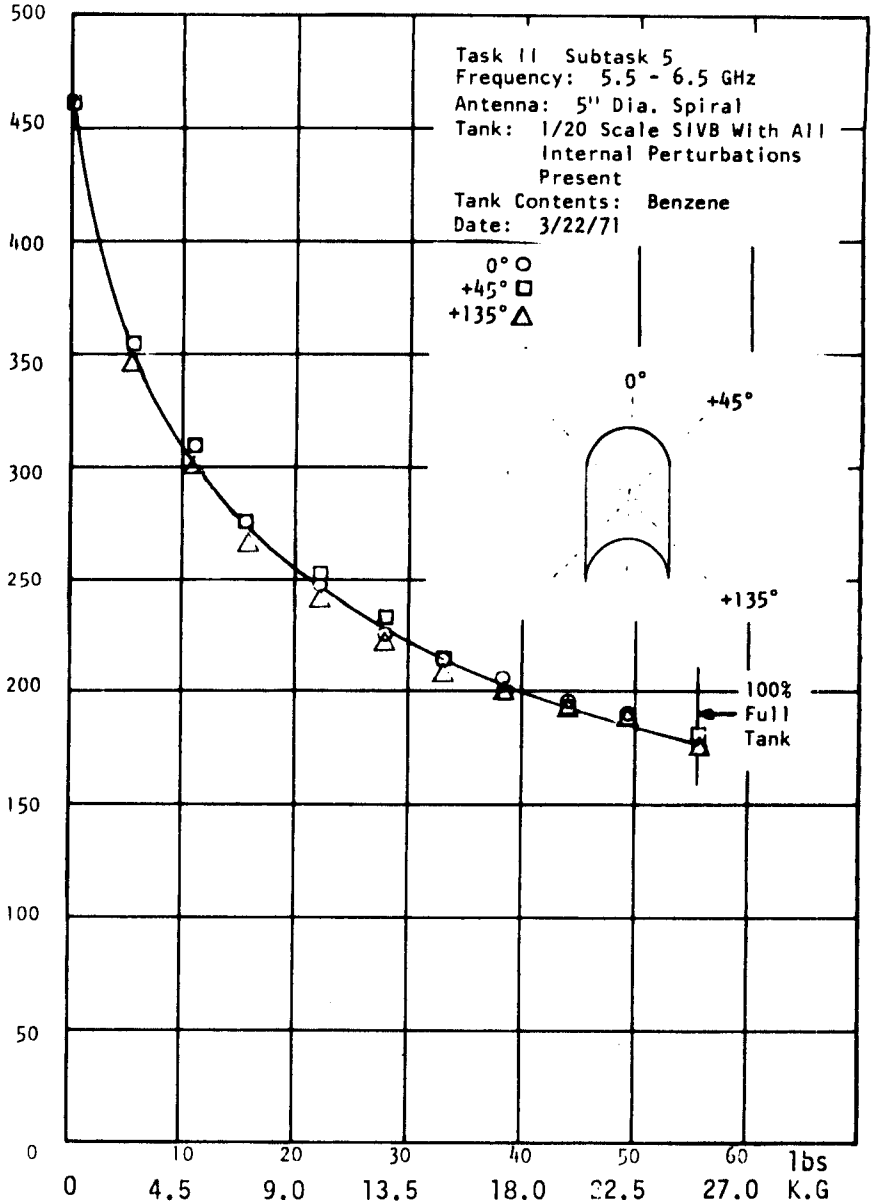

Figure 5.- BENZENE MASS

LOX loading data can be seen in Figures 6 and 7 for two different tank geometries and Liquid Nitrogen loading data can be seen in Figure 8, and LOX data of a different frequency in Figure 9. The low loss characteristics of LN_2 make it more suitable to gaging with an ascending mode count as the quantity increases. High loss fluids are generally more suitable to decreasing slope or decreasing mode count with increasing mass.

The tank probe used to gather the Benzene data can be seen in Figure 10. The tank, a 1/20 scale LH_2 tank can be seen in Figure 11 with the top dome shown in Figure 12.

The top dome of a 1/10 scale SIVB LH_2 tank, used for LOX and LN_2 tests can be seen in Figure 13 with RF probe installed. The tank probe ready for installation can be seen in Figure 14. Figure 15 shows the packaged electronics (RF section at the left and electronic processor section at the right) for a recent breadboard system.

Error Analysis

With the present state of low level sophistication in the prototype systems tested, the repeatable accuracy of the spiral antenna and breadboard electronics is as follows:

0 - 30% fill $\pm$ 1%
30 - 50% fill $\pm$ 1.5%
50 - 70% Fill $\pm$ 1.8%
70 - 100% Fill $\pm$ 2.7%

This accuracy is based on using 99% of the data points taken during testing of the latest breadboard system and compares the electronic processor output signal with the reading on the weighing scales 24 inch dial.

Methods are being studied to improve the accuracy at the full end by mode count feedback loops to change the RF input frequency to improve the full end sensitivity. The objective is 1.5% maximum error (% of full reading) from empty to full.

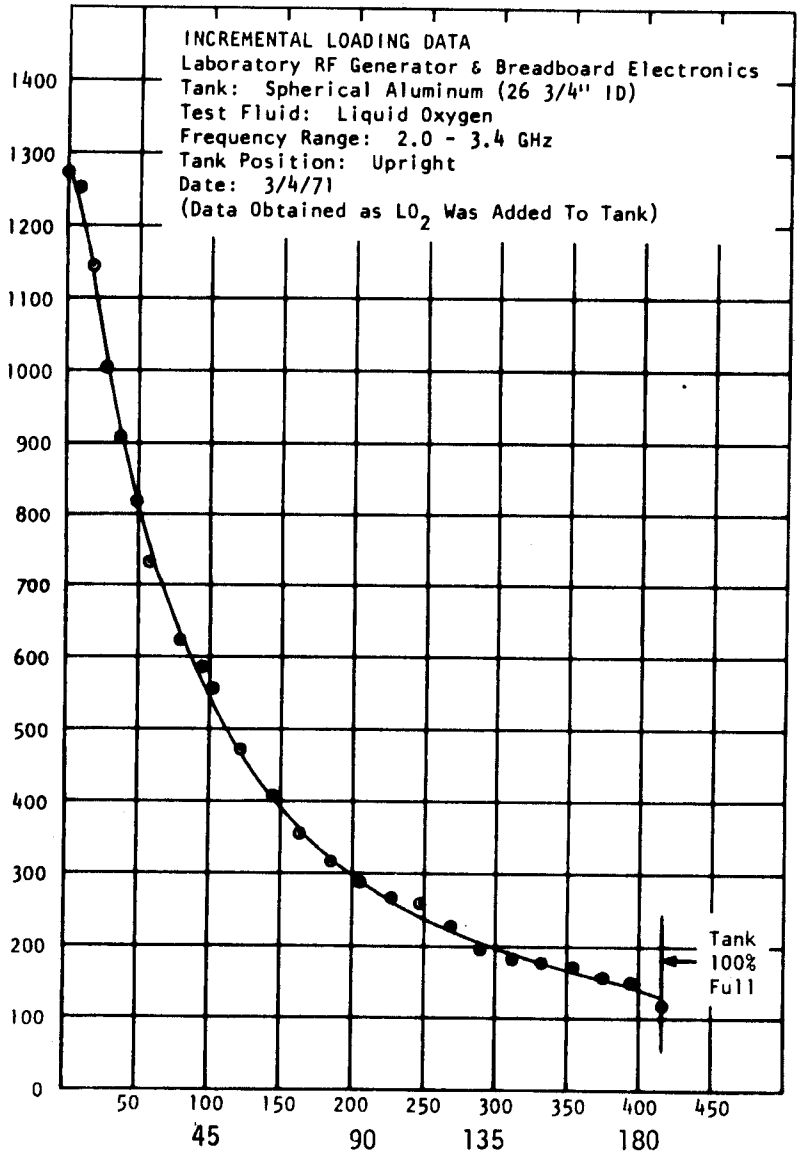

Figure 6.- LOX MASS

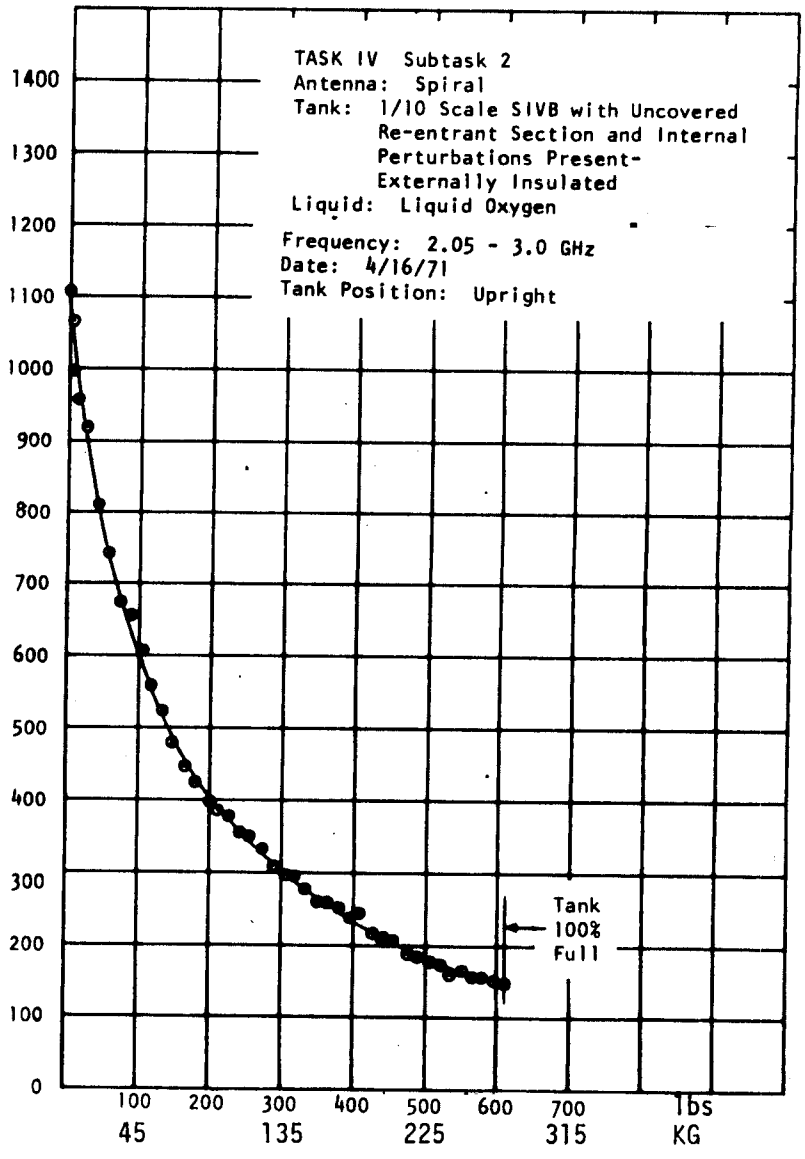

Figure 7.- LOX MASS

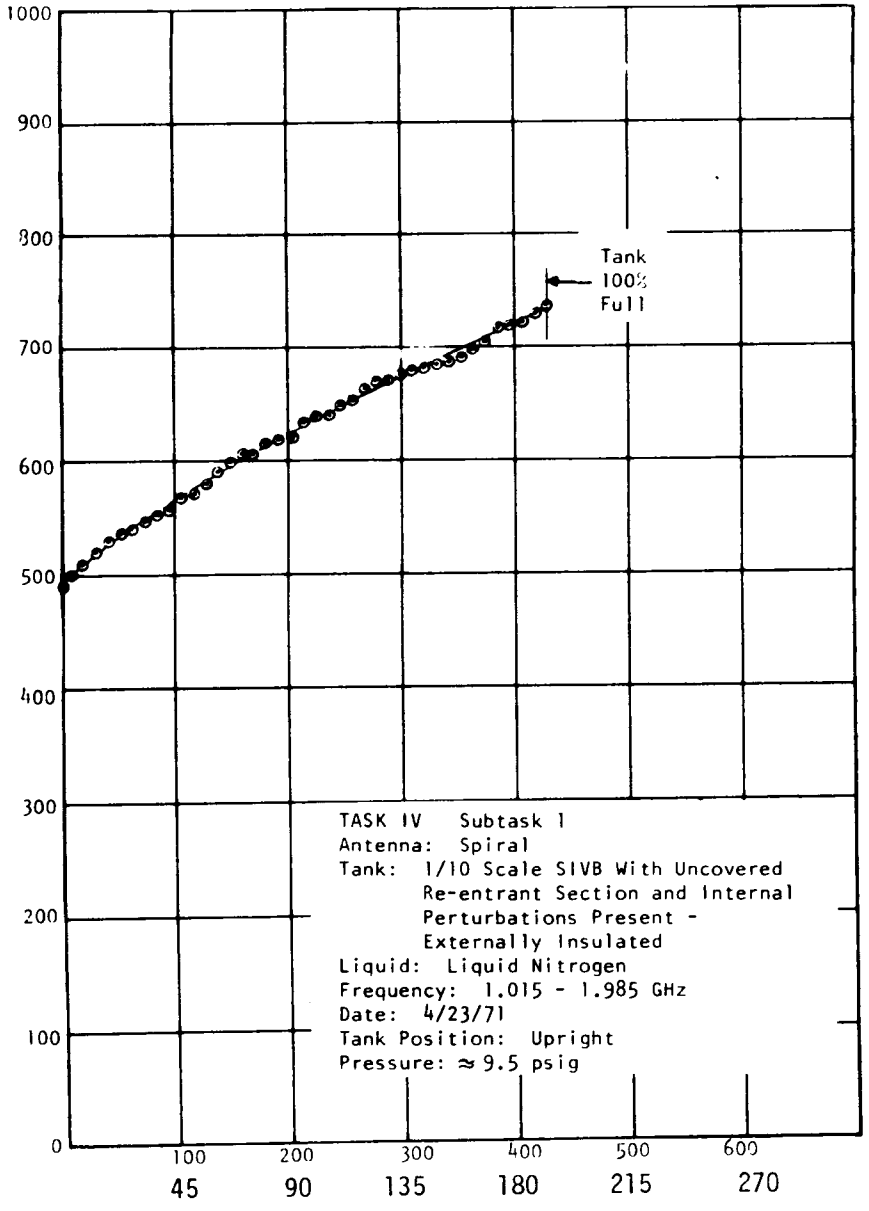

Figure 8.- LN_2 MASS

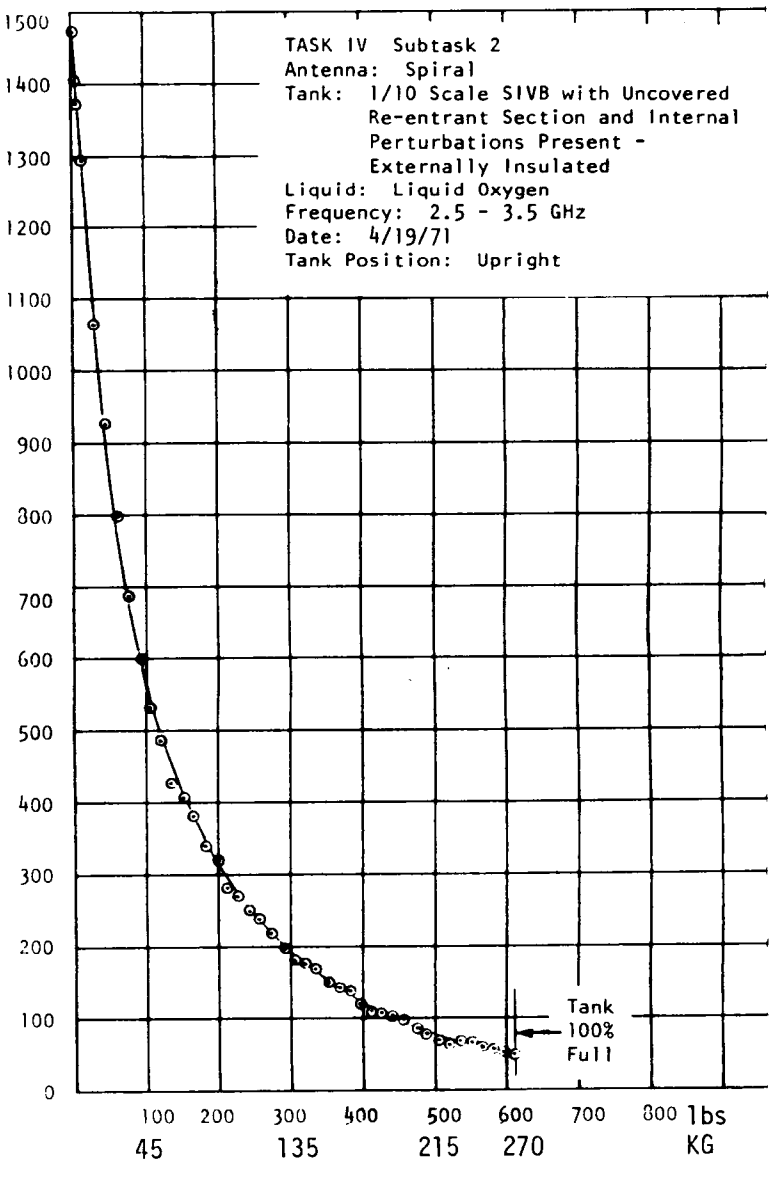

Figure 9.- LOX MASS

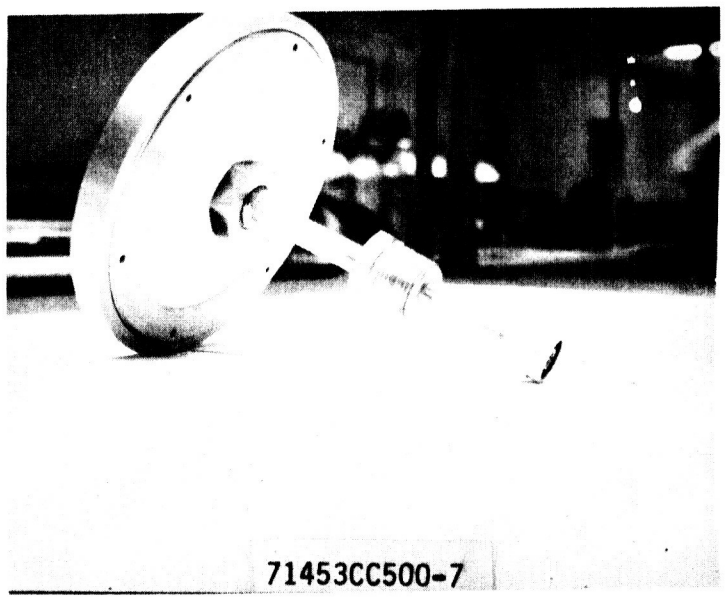

Figure 10.- RF GAGING PROBE COMPLETED READY FOR INSTALLATION IN THE 1/10 SCALE SIVB TANK

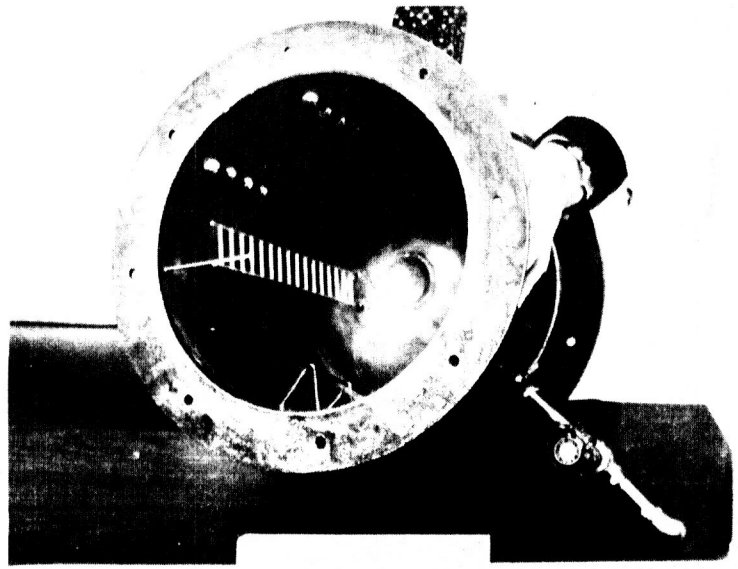

Figure 11.- 1/20 SCALE SIVB TANK USED FOR RF GAGING STUDIES WITH J-2 TEST STAND INTERNAL HARDWARE

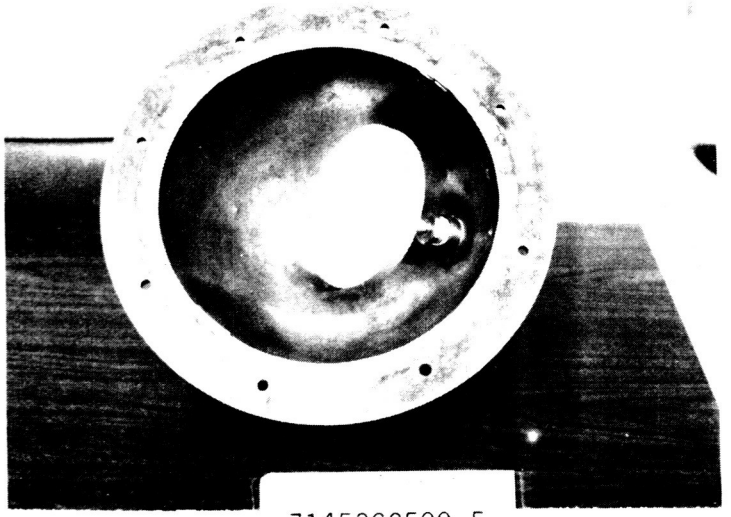

71453CC500-5

Figure 12.- 1/20 SCALE TANK DOME WITH PROBE INSTALLED

71453CC116-1

Figure 13.- 1/10 SCALE SIVB TANK TEST SETUP FOR BENZENE GAGING TESTS

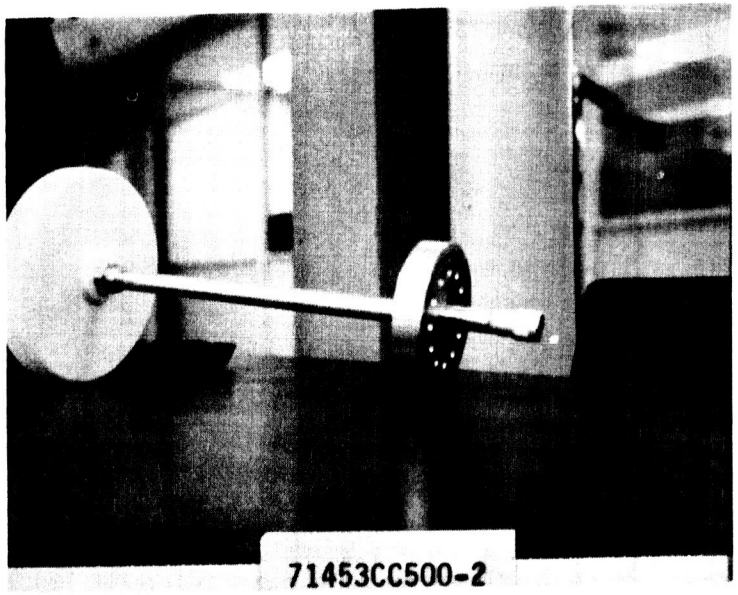

Figure 14.- RF GAGING PROBE USED FOR 1/10 SCALE SYSTEM CRYOGENIC TEST

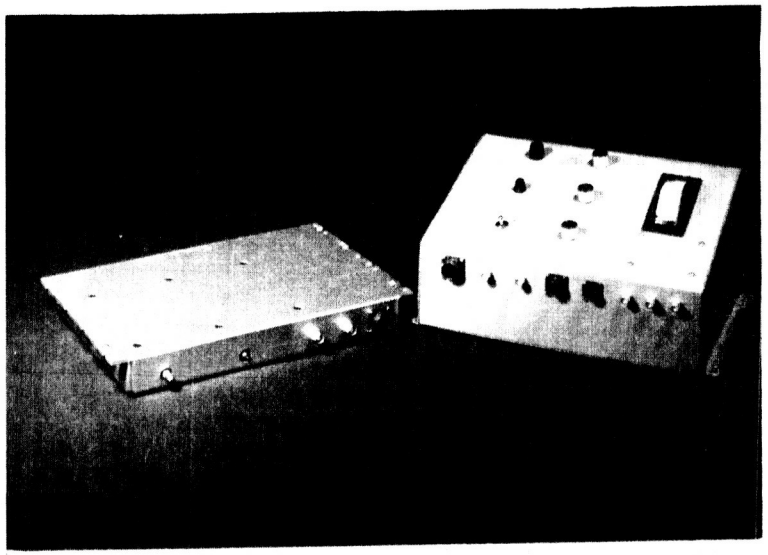

Figure 15.- PACKAGED ELECTRONICS (BREADBOARD) TYPICAL FOR 1/10 SCALE SIVB SYSTEM

CONCLUSIONS

Test Results and Analytical Data now available lead to the following conclusions:

1) The RF Gaging technique has been proven feasible for both cryogenic fluids such as LOX, and for various non-cryogenic dielectric fluids.

2) RF Gaging technology has advanced to a point where the performance of the system can be predicted for most types of spacecraft tanks and fluids. Scaling laws have been developed which permit the prediction of operating characteristics of the RF Gaging System when used with full-size shuttle vehicle type tanks.

3) Solid state RF hardware is now available for construction of ground test and flight test systems and allows more direct fabrication and tests of breadboard systems for performance and accuracy evaluations.